ASYMMETRIC BEAMPATTERNS WITH CIRCULAR DIFFERENTIAL MICROPHONE ARRAYS

Yaakov Buchris and Israel Cohen

Technion, Israel Institute of Technology
Technion City, Haifa 32000, Israel
{bucris@campus, icohen@ee}.technion.ac.il

Jacob Benesty

INRS-EMT, University of Quebec
800 de la Gauchetiere Ouest, Suite 6900
Montreal, QC H5A 1K6, Canada
benesty@emt.inrs.ca

ABSTRACT

Circular differential microphone arrays (CDMAs) facilitate compact superdirective beamformers whose beampatterns are nearly frequency invariant, and allow perfect steering for all azimuthal directions. Herein, we eliminate the inherent limitation of symmetric beampatterns associated with a linear geometry, and introduce an analytical asymmetric model for Nth-order CDMAs. We derive the theoretical asymmetric beampattern, and develop the asymmetric supercardioid. In addition, an Nth-order CDMAs design is presented based on the mean-squared-error (MSE) criterion. Experimental results show that the proposed model yields optimal performance in terms of white noise gain, directivity factor, and front-to-back ratio, as well as more flexible nulls design for the interfering signals.

Index Terms— Circular differential microphone arrays, asymmetric beampatterns, broadband beamforming, supercardioid.

1. INTRODUCTION

Differential microphone arrays (DMAs) beamforming constitute a promising solution to some real-world applications involving speech signals, e.g., hands-free telecommunication [1]. DMAs refer to arrays that combine closely spaced sensors to respond to the spatial derivatives of the acoustic pressure field. These small-size arrays yield nearly frequency-invariant beampatterns, and include the superdirective beamformer [2, 3] as a particular case.

The modern concept of DMAs employs pressure microphones, and digital signal processing techniques are used to obtain desired directional response [4–8]. Most of the work on DMAs deals with a linear array geometry, which is preferable in some applications involving small devices. Yet, linear arrays may not have the same response at different directions, and are less suitable for applications like 3D sound recording where signals may come from any direction. In such cases, circular arrays are advantageous [9–13].

Previous works on DMAs, both for linear and circular geometries (e.g., [14, 15]), have considered only the case of symmetric beampatterns, which is an inherent limitation of the linear geometry. Yet, in different array geometries like the circular geometry, asymmetric design may lead to substantial performance improvement.

In this paper, we derive an analytical model for asymmetric circular differential microphone arrays (CDMAs) which includes also the traditional symmetric model as a particular case. It is shown that an asymmetric model achieves higher performances in terms of white noise gain (WNG), directivity factor (DF), and front-to-back-ratio (FBR) due to a more flexible design, which can better take into account the constraints regarding the null directions. We first derive the analytical asymmetric beampattern and then derive an asymmetric version for the supercardioid which is designed to maximize the FBR [4]. Additionally, a mean-squared-error (MSE) solution for an Nth-order CDMA is developed, which enables perfect steering to every azimuthal direction. In the simulations section, we present a third-order asymmetric design and demonstrate its benefits with respect to the symmetric one.

This research was supported by the Israel Science Foundation (grant no. 576/16), Qualcomm Research Fund and MAFAAT-Israel Ministry of Defense.

2. SIGNAL MODEL

We consider an acoustic source signal, $X(\omega)$, that propagates in an anechoic acoustic environment at the speed of sound, i.e., $c \approx 340$ m/s, and impinges on a uniform circular array (UCA) of radius r, consisting of M omnidirectional microphones, where the distance between two successive sensors is equal to

$$\delta = 2r \sin\left(\frac{\pi}{M}\right) \approx \frac{2\pi r}{M}. \quad (1)$$

The direction of $X(\omega)$ to the array is denoted by the azimuth angle $\theta_{\rm s}$, measured anti-clockwise from the x axis, i.e., at $\theta = 0^\circ$. Assuming far-field propagation, the time delay between the mth microphone and the center of the array is $\tau_m(\theta_{\rm s}) = \frac{r}{c}\cos(\theta_{\rm s} - \psi_m)$, $m = 1, 2, ..., M$, where $\psi_m = \frac{2\pi(m-1)}{M}$ is the angular position of the mth array element. The mth microphone signal is

$$Y_m(\omega) = e^{j\varpi\cos(\theta_{\rm s}-\psi_m)}X(\omega) + V_m(\omega),\ m = 1, 2, ..., M, \quad (2)$$

where $\varpi = \frac{\omega r}{c}$, $j = \sqrt{-1}$, $\omega = 2\pi f$ is the angular frequency, $f > 0$ is the temporal frequency, and $V_m(\omega)$ is the additive noise at the mth microphone. In a vector form, (2) becomes

$$\mathbf{y}(\omega) = [Y_1(\omega)\ \cdots\ Y_M(\omega)]^T = \mathbf{d}\left(\omega, \theta_{\rm s}\right)X(\omega) + \mathbf{v}(\omega), \quad (3)$$

where $\mathbf{d}\left(\omega, \theta_{\rm s}\right)$ is the steering vector at $\theta = \theta_{\rm s}$, i.e.,

$$\mathbf{d}\left(\omega, \theta_{\rm s}\right) = \left[e^{j\varpi\cos(\theta_{\rm s}-\psi_1)} \cdots e^{j\varpi\cos(\theta_{\rm s}-\psi_M)}\right]^T, \quad (4)$$

the superscript ^{T} is the transpose operator, the vector $\mathbf{v}(\omega)$ is defined similarly to $\mathbf{y}(\omega)$, and the acoustic wavelength is $\lambda = c/f$. It is assumed that the element spacing, δ, is much smaller than the wavelength of the incoming signal, i.e, $\delta \ll \lambda$, in order to approximate the differential of the pressure signal.

Assuming a 2D scenario, the frequency-invariant beampattern of an Nth-order DMA is given, for any steering angle $\theta_{\rm s}$, as [4]

$$\mathcal{B}_N(\theta-\theta_{\rm s})=\sum_{n=0}^{N}a_{N,n}\cos^n(\theta-\theta_{\rm s}), \tag{5}$$

where θ is the azimuth, and $\{a_{N,n}\}_{n=0}^{N}$ are real coefficients. The beampattern $\mathcal{B}_N(\theta-\theta_{\rm s})$ is a symmetric function which can properly describe the frequency-invariant beampattern of linear DMAs. Herein, we derive an asymmetric model for Nth-order CDMAs.

3. ASYMMETRIC BEAMPATTERN FOR CDMAs

We start with a simple first-order asymmetric case and then generalize it for any order, N. First-order CDMAs can be designed with at least three microphones, whose positions are $\psi_1=0,\psi_2=\frac{2\pi}{3}$, and $\psi_3=\frac{4\pi}{3}$. Assuming a 2D scenario, the acoustic propagation field received at each sensor is

$$p\left(k,r,\theta,\psi_m\right)=P_0e^{j\varpi\cos(\theta-\psi_m)},\ \ m=1,2,3, \tag{6}$$

where P_0 is the wave amplitude, and $k=\frac{\omega}{c}$ is the wave number. By adding a gain $a_me^{j\omega\tau_m}$ at each sensor, and summing all the sensors, we get the output power:

$$p_{\rm out}\left(k,r,\theta\right)=P_0\sum_{m=1}^{3}a_me^{j\omega\tau_m}e^{j\varpi\cos(\theta-\psi_m)}, \tag{7}$$

where a_m is a real number and τ_m is a temporal delay added to the signal acquired by the mth microphone. Without loss of generality, we assume that $P_0=1$, $a_1=1$, and $\tau_1=0$. Using the approximation $e^x\approx1+x$, and due to the model assumption $\delta\ll\lambda$, (7) becomes

$$\begin{aligned}p_{\rm out}\left(k,r,\theta\right)&\approx1+a_2+a_3\\&\quad+j\omega\sum_{m=1}^{3}a_m\left[\tau_m+\frac{r}{c}\cos(\theta-\psi_m)\right].\end{aligned} \tag{8}$$

In order to simplify (8), we impose $a_2+a_3=-1$, and define

$$\begin{aligned}\alpha_1&=\frac{\sum_{m=1}^{3}a_m\tau_m}{\sum_{m=1}^{3}a_m\left(\tau_m+\frac{r}{c}\cos\psi_m\right)},\\1-\alpha_1&=\frac{\sum_{m=1}^{3}a_m\frac{r}{c}\cos\psi_m}{\sum_{m=1}^{3}a_m\left(\tau_m+\frac{r}{c}\cos\psi_m\right)},\\\beta_1&=\frac{\sum_{m=1}^{3}a_m\frac{r}{c}\sin\psi_m}{\sum_{m=1}^{3}a_m\left(\tau_m+\frac{r}{c}\cos\psi_m\right)}.\end{aligned} \tag{9}$$

Now we can get the normalized response of the first-order asymmetric CDMA:

$$\mathcal{B}_1\left(\theta\right)=\frac{p_{\rm out}\left(k,r,\theta\right)}{p_{\rm out}\left(k,r,0\right)}=\alpha_1+(1-\alpha_1)\cos\theta+\beta_1\sin\theta. \tag{10}$$

The second-order asymmetric CDMA's beampattern can be written as a product of two first-order asymmetric beampatterns terms, i.e.,

$$\mathcal{B}_2\left(\theta\right)=\prod_{i=1}^{2}\left[\alpha_i+(1-\alpha_i)\cos\theta+\beta_i\sin\theta\right], \tag{11}$$

from which, we can easily derive the general form of the second-order asymmetric CDMA:

$$\mathcal{B}_2\left(\theta\right)=\upsilon_0+\upsilon_1\cos\theta+\upsilon_2\cos^2\theta+\upsilon_3\sin\theta\cos\theta+\upsilon_4\sin\theta, \tag{12}$$

where $\{\upsilon_i\}_{i=0}^{4}$ are real coefficients which depend on $\{\alpha_i,\beta_i\}_{i=1}^{2}$. Similarly, the third-order asymmetric beampattern is

$$\begin{aligned}\mathcal{B}_3\left(\theta\right)&=\epsilon_0+\epsilon_1\cos\theta+\epsilon_2\cos^2\theta+\epsilon_3\cos^3\theta\\&\quad+\epsilon_4\sin\theta\cos\theta+\epsilon_5\sin\theta+\epsilon_6\sin^3\theta.\end{aligned} \tag{13}$$

Based on the last results, we can obtain the Nth-order asymmetric CDMAs beampattern with the mainlobe steered to $\theta_{\rm s}$:

$$\begin{aligned}\mathcal{B}_N\left(\theta-\theta_{\rm s}\right)&=\sum_{n=0}^{N}\xi_n\cos^n(\theta-\theta_{\rm s})+\sum_{n=0}^{\lfloor\frac{N-1}{2}\rfloor}\mu_n\sin^{2n+1}(\theta-\theta_{\rm s})\\&\quad+\sum_{n=1}^{\lfloor\frac{N}{2}\rfloor}\zeta_n\cos(\theta-\theta_{\rm s})\sin^{2n-1}(\theta-\theta_{\rm s}),\end{aligned} \tag{14}$$

which is a trigonometric polynomial of power N with $2N$ roots. In fact, (14) can be equivalently expressed as [16]

$$\mathcal{B}_N\left(\theta-\theta_{\rm s}\right)=\sum_{n=0}^{N}a_n\cos\left[n(\theta-\theta_{\rm s})\right]+\sum_{n=1}^{N}b_n\sin\left[n(\theta-\theta_{\rm s})\right]. \tag{15}$$

4. OPTIMAL ASYMMETRIC SUPERCARDIOID

The common directivity patterns in the context of microphone arrays are dipole, cardioid, hypercardioid, and supercardioid. These patterns, originally developed for linear geometry, are traditionally symmetric with respect to the steering angle, $\theta_{\rm s}$.

In this section, we develop an asymmetric version of the supercardioid for CDMAs. The supercardioid pattern maximizes the FBR [4], which is defined for a cylindrical noise field as

$$\mathcal{F}=\frac{\int_{-\pi/2}^{\pi/2}\mathcal{B}_N^2\left(\theta\right)d\theta}{\int_{\pi/2}^{3\pi/2}\mathcal{B}_N^2\left(\theta\right)d\theta}, \tag{16}$$

where we assume, without loss of generality, that the steering angle is $\theta_{\rm s}=0^\circ$. It is easily seen that $\int_{-\pi/2}^{\pi/2}\mathcal{B}_N^2\left(\theta\right)d\theta=\mathbf{c}^T\mathbf{\Gamma}_{\rm f}\mathbf{c}$ and $\int_{\pi/2}^{3\pi/2}\mathcal{B}_N^2\left(\theta\right)d\theta=\mathbf{c}^T\mathbf{\Gamma}_{\rm b}\mathbf{c}$, where

$$\mathbf{c}=\left[a_0,a_1,...,a_N,b_1,...,b_N\right]^T \tag{17}$$

is a vector of length $2N+1$ containing the coefficients of the asymmetric beampattern (15). Matrices $\mathbf{\Gamma}_{\rm f}$ and $\mathbf{\Gamma}_{\rm b}$ are diagonal, with

$$\begin{aligned}\left[\mathbf{\Gamma}_{\rm f}\right]_{n,n}&=\begin{cases}\int_{-\pi/2}^{\pi/2}\cos^2\left(n\theta\right)d\theta, & n=0,1,...,N\\\int_{-\pi/2}^{\pi/2}\sin^2\left[(n-N)\theta\right]d\theta, & n=N+1,...,2N\end{cases}\\\left[\mathbf{\Gamma}_{\rm b}\right]_{n,n}&=\begin{cases}\int_{\pi/2}^{3\pi/2}\cos^2\left(n\theta\right)d\theta, & n=0,1,...,N\\\int_{\pi/2}^{3\pi/2}\sin^2\left[(n-N)\theta\right]d\theta, & n=N+1,...,2N.\end{cases}\end{aligned} \tag{18}$$

The coefficients $\{a_n\}_{n=0}^{N}$ and $\{b_n\}_{n=1}^{N}$ are independent by the diagonality of $\mathbf{\Gamma}_{\rm f}$ and $\mathbf{\Gamma}_{\rm b}$. Thus, the circular geometry provides more degrees of freedom in the design of optimal patterns such as

the supercardioid, and more directional constraints should be imposed. The first one is the distortionless constraint:

$$\mathcal{B}_N\left(\theta_{\rm s}=0^\circ\right)=1, \tag{19}$$

leading to $\sum_{n=0}^{N} a_n = 1$. We can add up to $L \leq 2N$ attenuation constraints of the form:

$$\mathcal{B}_N\left(\theta=\theta_l\right)=g_l,\ \ l=1,2,...,L, \tag{20}$$

where $0 \leq g_l \leq 1$. We formulate these constraints as

$$\mathbf{H}_{\rm c}\mathbf{c}=\mathbf{g}, \tag{21}$$

where $\mathbf{H}_{\rm c}$ is the constraint matrix of size $(L+1)\times(2N+1)$, typically non-diagonal. Vector $\mathbf{g}$ of length $L+1$ contains the coefficients $g_l,\ l=1,2,...,L$, and a single unity entry, satisfying (19).

We can now formulate the optimization problem:

$$\max_{\mathbf{c}} \frac{\mathbf{c}^T\mathbf{\Gamma}_{\rm f}\mathbf{c}}{\mathbf{c}^T\mathbf{\Gamma}_{\rm b}\mathbf{c}}, \quad \text{subject to } \mathbf{H}_{\rm c}\mathbf{c}=\mathbf{g}. \tag{22}$$

Rather than solving (22), we solve the equivalent problem:

$$\max_{\hat{\mathbf{c}}} \frac{\hat{\mathbf{c}}^T\hat{\mathbf{\Gamma}}_{\rm f}\hat{\mathbf{c}}}{\hat{\mathbf{c}}^T\hat{\mathbf{\Gamma}}_{\rm b}\hat{\mathbf{c}}} \quad \text{subject to } \hat{\mathbf{H}}_{\rm c}\hat{\mathbf{c}}=\mathbf{0}, \tag{23}$$

where

$$\hat{\mathbf{c}}=\begin{bmatrix}\mathbf{c}\\ -1\end{bmatrix},\ \hat{\mathbf{H}}_{\rm c}=\begin{bmatrix}\mathbf{H}_{\rm c} & \mathbf{g}\end{bmatrix},\ \hat{\mathbf{\Gamma}}_{\rm f}=\begin{bmatrix}\mathbf{\Gamma}_{\rm f} & \mathbf{0}\\ \mathbf{0}^T & 0\end{bmatrix},\ \hat{\mathbf{\Gamma}}_{\rm b}=\begin{bmatrix}\mathbf{\Gamma}_{\rm b} & \mathbf{0}\\ \mathbf{0}^T & 0\end{bmatrix}. \tag{24}$$

Let $\mathbf{D}$ be a null-space matrix of $\hat{\mathbf{H}}_{\rm c}$ (i.e., $\hat{\mathbf{H}}_{\rm c}\mathbf{D}=\mathbf{0}$) of size $(2N+2)\times(2N+1-L)$ and rank of $2N+1-L$, which contains $2N+1-L$ basis vectors in its columns, and let $\hat{\mathbf{c}}=\mathbf{D}\tilde{\mathbf{c}}$. Note that the matrices $\mathbf{D}^T\hat{\mathbf{\Gamma}}_{\rm f}\mathbf{D}$ and $\mathbf{D}^T\hat{\mathbf{\Gamma}}_{\rm b}\mathbf{D}$ are full-rank even though $\hat{\mathbf{\Gamma}}_{\rm f}$ and $\hat{\mathbf{\Gamma}}_{\rm b}$ are not full rank since the product matrices $\mathbf{D}^T\hat{\mathbf{\Gamma}}_{\rm f}\mathbf{D}$ and $\mathbf{D}^T\hat{\mathbf{\Gamma}}_{\rm b}\mathbf{D}$ are of size $(2N+1-L)\times(2N+1-L)$ with a rank of $(2N+1-L)$, i.e, full-rank matrices. Thus, we transform (23) to the following unconstrained optimization problem [17]:

$$\max_{\tilde{\mathbf{c}}} \frac{\tilde{\mathbf{c}}^T\mathbf{D}^T\hat{\mathbf{\Gamma}}_{\rm f}\mathbf{D}\tilde{\mathbf{c}}}{\tilde{\mathbf{c}}^T\mathbf{D}^T\hat{\mathbf{\Gamma}}_{\rm b}\mathbf{D}\tilde{\mathbf{c}}}. \tag{25}$$

The solution to (25) is the generalized eigenvector of $\mathbf{D}^T\hat{\mathbf{\Gamma}}_{\rm f}\mathbf{D}$ and $\mathbf{D}^T\hat{\mathbf{\Gamma}}_{\rm b}\mathbf{D}$ that corresponds to the maximal generalized eigenvalue, i.e.,

$$\mathbf{D}^T\hat{\mathbf{\Gamma}}_{\rm f}\mathbf{D}\tilde{\mathbf{c}}_{\rm opt}=\lambda_{\max}\mathbf{D}^T\hat{\mathbf{\Gamma}}_{\rm b}\mathbf{D}\tilde{\mathbf{c}}_{\rm opt}, \tag{26}$$

Finally, we reconstruct $\mathbf{c}$ from $\tilde{\mathbf{c}}_{\rm opt}$.

5. DESIGN FOR ASYMMETRIC CDMAs

We now proceed to design the beamformer. For that, the signal of each microphone is multiplied by a complex gain $H_m(\omega),\ m=1,2,...,M$. Then, all the signals are summed to form the beamformer output. The beampattern is defined as

$$\mathcal{B}\left[\mathbf{h}(\omega),\theta\right]=\mathbf{h}^H(\omega)\mathbf{d}(\omega,\theta), \tag{27}$$

where

$$\mathbf{h}(\omega)=\left[H_1(\omega)\ \ H_2(\omega)\ \ \cdots\ \ H_M(\omega)\right]^T. \tag{28}$$

While (27) is the designed asymmetric beampattern, (15) is the analytical asymmetric beampattern which is considered as the desired beampattern.

Similarly to what have been done in [18], we would like to find a filter $\mathbf{h}(\omega)$, so that $\mathcal{B}\left[\mathbf{h}(\omega),\theta\right]$ is as close as possible to $\mathcal{B}_n\left(\theta\right)$ (15), in the MSE sense. Assuming $\theta_{\rm s}=0^\circ$, we can express (15) as

$$\mathcal{B}_N\left(\theta\right)=\mathbf{t}^T(\theta)\mathbf{a}+\mathbf{s}^T(\theta)\mathbf{b}, \tag{29}$$

where

$$\mathbf{t}(\theta)=\left[1\ \ \cos\theta\ \ \cdots\ \ \cos(N\theta)\right]^T, \tag{30}$$

$$\mathbf{s}(\theta)=\left[0\ \ \sin\theta\ \ \cdots\ \ \sin(N\theta)\right]^T, \tag{31}$$

$$\mathbf{a}=\left[a_0\ \ a_1\ \ \cdots\ \ a_N\right]^T, \tag{32}$$

$$\mathbf{b}=\left[b_0\ \ b_1\ \ \cdots\ \ b_N\right]^T, \tag{33}$$

are vectors of length $N+1$. From now on, it is assumed that θ is a real random variable, which is uniformly distributed in the interval $[0,2\pi]$. We define the MSE criterion between the array beampattern and the desired directivity pattern as

$$\begin{aligned}\mathrm{MSE}\left[\mathbf{h}(\omega)\right]&=E\left\{\left|\mathcal{B}\left[\mathbf{h}(\omega),\theta\right]-\mathcal{B}_N\left(\theta\right)\right|^2\right\}\\ &=\mathbf{h}^H(\omega)\mathbf{\Phi_d}\mathbf{h}(\omega)-\mathbf{h}^H(\omega)\left[\mathbf{\Phi_{dt}}\mathbf{a}+\mathbf{\Phi_{ds}}\mathbf{b}\right]\\ &-\left[\mathbf{a}^T\mathbf{\Phi}_{\mathbf{dt}}^H+\mathbf{b}^T\mathbf{\Phi}_{\mathbf{ds}}^H\right]\mathbf{h}(\omega)+\mathbf{a}^T\mathbf{\Phi_t}\mathbf{a}+\mathbf{b}^T\mathbf{\Phi_s}\mathbf{b}.\end{aligned} \tag{34}$$

where $E\left\{\cdot\right\}$ denotes mathematical expectation with respect to θ, $\mathbf{\Phi_d}=E\left[\mathbf{d}(\omega,\theta)\mathbf{d}^H(\omega,\theta)\right]$, $\mathbf{\Phi_{dt}}=E\left[\mathbf{d}(\omega,\theta)\mathbf{t}^T(\omega,\theta)\right]$, $\mathbf{\Phi_{ds}}=E\left[\mathbf{d}(\omega,\theta)\mathbf{s}^T(\omega,\theta)\right]$, $\mathbf{\Phi_t}=E\left[\mathbf{t}(\omega,\theta)\mathbf{t}^T(\omega,\theta)\right]$, and $\mathbf{\Phi_s}=E\left[\mathbf{s}(\omega,\theta)\mathbf{s}^T(\omega,\theta)\right]$.

To find the optimal filter in the MSE sense, it is important to minimize (34) subject to the distortionless constraint $\mathbf{d}^H\left(\omega,\theta_{\rm s}\right)\mathbf{h}(\omega)=1$, i.e.,

$$\min_{\mathbf{h}(\omega)}\ \mathrm{MSE}\left[\mathbf{h}(\omega)\right] \quad \text{subject to} \quad \mathbf{d}^H\left(\omega,\theta_{\rm s}\right)\mathbf{h}(\omega)=1. \tag{35}$$

The optimal solution is given by

$$\mathbf{h}_{\rm opt}(\omega)=\mathbf{h}_{\rm u}(\omega)+\frac{\left[1-\mathbf{d}(\omega,\theta_{\rm s})\mathbf{h}_{\rm u}\right]\mathbf{\Phi}_{\mathbf{ds}}^{-\mathbf{1}}(\omega)\mathbf{d}(\omega,\theta_{\rm s})}{\mathbf{d}^H(\omega,\theta_{\rm s})\mathbf{\Phi}_{\mathbf{d}}^{-\mathbf{1}}(\omega)\mathbf{d}(\omega,\theta_{\rm s})} \tag{36}$$

where $\mathbf{h}_{\rm u}(\omega)=\mathbf{\Phi}_{\mathbf{d}}^{-\mathbf{1}}(\omega)\left[\mathbf{\Phi_{dt}}(\omega)\mathbf{b}+\mathbf{\Phi_{ds}}(\omega)\mathbf{a}\right]$ is the unconstrained filter obtained by minimizing $\mathrm{MSE}\left[\mathbf{h}(\omega)\right]$.

6. A DESIGN EXAMPLE

In this section, we present a design example of the third-order asymmetric supercardioid. Third-order designs require at least $M=7$ microphones. Let us assume that the steering angle is $\theta_{\rm s}=0^\circ$ and we would like to impose three nulls at $\theta_1=75^\circ$, $\theta_2=105^\circ$ and $\theta_3=220^\circ$. We choose $r=0.75$ cm which leads to $\delta=0.65$ cm.

First, we need to find the corresponding analytical asymmetric beampattern. Solving (26), the optimal coefficients vector, $\mathbf{c}$ (17) is calculated and substituted into (15). The three additional roots are $\theta_4=150^\circ$, $\theta_5=194^\circ$, and $\theta_6=260^\circ$. Figure 1 shows the analytical beampattern of the third-order asymmetric design (blue solid line), its symmetric version (black dashed line), i.e., the beampattern for the case that $\theta_4=140^\circ$, $\theta_5=255^\circ$, and $\theta_6=285^\circ$, and also the third-order unconstrained symmetric supercardioid (red circles line), which was derived in [4] and obtained for nulls at

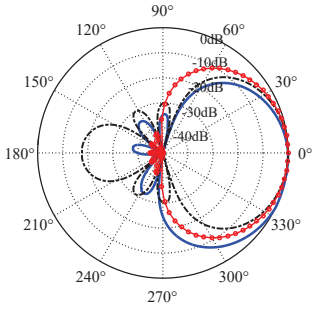

Figure 1: Beampattern for the third-order asymmetric supercardioid (blue solid line) and its symmetric version (black dashed line). The red circles line is the unconstrained third-order symmetric supercardioid [4]. $\theta_1 = 75^\circ$, $\theta_2 = 105^\circ$, $\theta_3 = 220^\circ$.

$\theta_1 = 98^\circ$, $\theta_2 = 125^\circ$ and $\theta_3 = 161^\circ$, and their symmetric directions. The latter is obtained by direct optimization of the FBR without any constraints on the null directions.

Using the calculated values of $\mathbf{c}$ (17) and of $\{\theta_i\}_{i=1}^{6}$, we can calculate (36) and design the third-order asymmetric CDMA. Figure 2 shows the beampattern of the third-order asymmetric supercardioid (a),(d), the third-order symmetric supercardioid (b),(e), and the third-order unconstrained symmetric supercardioid (c),(f), for different frequencies and steering angles. The black dashed line is the designed beampattern (27), while the blue circles line is the analytical beampattern (15).

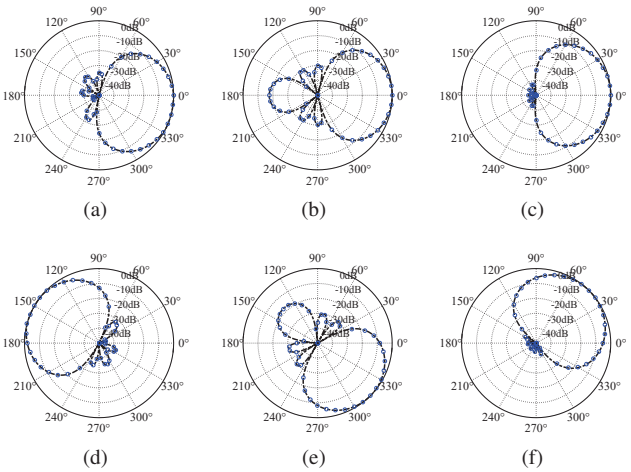

Figure 2: Beampatterns for the third-order asymmetric supercardioid CDMAs with $M = 7$ sensors and three imposed nulls for different steering angles and frequencies: (a) $\theta_s = 0^\circ$, $f = 1000$ Hz, (d) $\theta_s = 165^\circ$, $f = 1800$ Hz. Beampatterns of the corresponding third-order symmetric design: (b) $\theta_s = 0^\circ$, $f = 200$ Hz, (e) $\theta_s = 315^\circ$, $f = 2200$ Hz . Beampatterns of the third-order unconstrained symmetric supercardioid: (c) $\theta_s = 0^\circ$, $f = 1500$ Hz, (f) $\theta_s = 43^\circ$, $f = 3000$ Hz. The black dashed line is the designed beampattern (27), while the blue circles line is the analytical beampattern (15).

Figure 3 shows the WNG, the DF, and the FBR as a function of frequency for the third-order asymmetric supercardioid (blue solid line), the third-order symmetric supercardioid (black dashed line), and the third-order unconstrained symmetric supercardioid (red circles line). The WNG, the DF, and the FBR are defined as [14, ch.2]

$$\mathcal{W}\left[\mathbf{h}(\omega)\right] = \frac{\left|\mathbf{h}^H(\omega)\mathbf{d}(\omega,\theta_s)\right|^2}{\mathbf{h}^H(\omega)\mathbf{h}(\omega)}, \quad (37)$$

$$\mathcal{D}\left[\mathbf{h}(\omega)\right] = \frac{\left|\mathbf{h}^H(\omega)\mathbf{d}(\omega,\theta_s)\right|^2}{\mathbf{h}^H(\omega)\mathbf{\Gamma}_{\rm dn}(\omega)\mathbf{h}(\omega)}, \quad (38)$$

$$\mathcal{F}\left[\mathbf{h}(\omega)\right] = \frac{\int_{-\pi/2}^{\pi/2} \mathcal{B}^2[\mathbf{h}(\omega),\theta]d\theta}{\int_{\pi/2}^{3\pi/2} \mathcal{B}^2[\mathbf{h}(\omega),\theta]d\theta}, \quad (39)$$

where $\left[\mathbf{\Gamma}_{\rm dn}(\omega)\right]_{ij} = \text{sinc}\left(2\varpi\left|\sin\left[\frac{\pi(i-j)}{M}\right]\right|\right)$.

The performance of the asymmetric design is very similar to that of the unconstrained supercardioid in terms of WNG, DF, and FBR while the symmetric design achieves much lower FBR but slightly higher DF, due to a narrower mainlobe. In [16], we derive also the asymmetric hypercardioid and show that the asymmetric design can achieve superior performance also in terms of DF. In addition, practical methods to improved the WNG, based either on regularization methods or increasing the number of sensors, can be found in [19].

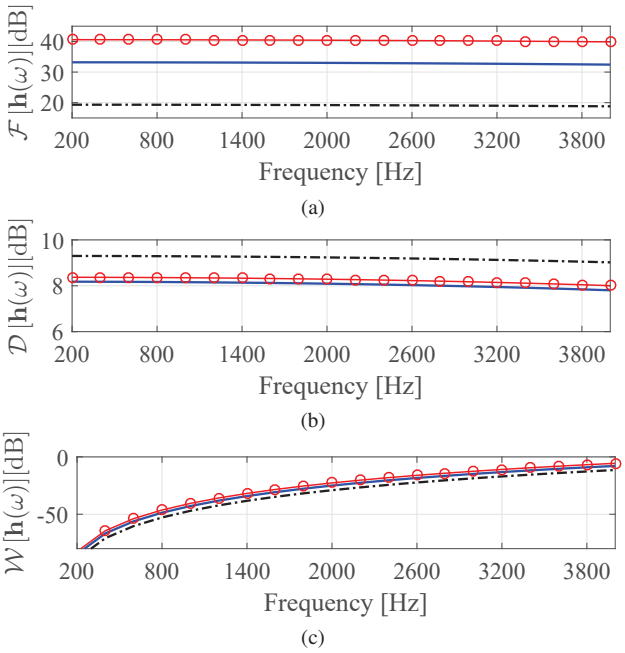

Figure 3: FBR (a), DF (b), and WNG (c) vs. frequency for the third-order asymmetric supercardioid (blue solid line), the third-order symmetric design (black dashed line), and the third-order unconstrained symmetric supercardioid (red circles line) with $M = 7$ sensors.

7. CONCLUSIONS

We have presented an analytical model for asymmetric CDMAs, which includes the traditional symmetric model as a particular case. We have derived an analytical model for Nth-order asymmetric beampattern, and asymmetric version of the supercardioid. A practical design of an Nth-order asymmetric beamformer for a given number of microphones, based on the MSE criteria, is also proposed. Simulation results show that the asymmetric model allows more degrees of freedom, compared to a symmetric model, which can be exploited for better FBR.

8. REFERENCES

[1] J. Benesty, J. Chen, and Y. Huang, *Microphone Array Signal Processing*. Berlin, Germany: Springer-Verlag, 2008.

[2] H. Cox, R. M. Zeskind, and T. Kooij, "Practical supergain," *IEEE Trans. Acoust., Speech, Signal Processing*, vol. ASSP-34, no. 3, pp. 393–397, June 1986.

[3] M. Crocco and A. Trucco, "Design of robust superdirective arrays with a tunable tradeoff between directivity and frequency-invariance," *IEEE Trans. Signal Process.*, vol. 59, no. 5, pp. 2169–2181, May 2011.

[4] G. W. Elko, "Superdirectional microphone arrays," in *Acoustic Signal Processing for Telecommunication*, S. L. Gay and J. Benesty, Eds. Boston, MA: Kluwer Academic Publishers, 2000, ch. 10, pp. 181–237.

[5] T. D. Abhayapala and A. Gupta, "Higher order differential-integral microphone arrays," *J. Acoust. Soc. Amer.*, vol. 127, pp. 227–233, May 2010.

[6] J. Benesty and J. Chen, *Study and Design of Differential Microphone Arrays*. Berlin, Germany: Springer-Verlag, 2012.

[7] E. De Sena, H. Hacihabibğlu, and Z. Cavetković, "On the design and implementation of higher order differential microphones," *IEEE Trans. Audio, Speech, Language Process.*, vol. 20, no. 1, pp. 162–174, Jan. 2012.

[8] Y. Buchris, I. Cohen, and J. Benesty, "First-order differential microphone arrays from a time-domain broadband perspective," in *International Workshop on Acoustic Echo and Noise Control (IWAENC) 2016 conf.*

[9] H. Teutsch and W. Kellerman, "Acoustic source detection and localization based on wavefield decomposition using circular microphone arrays," *J. Acoust. Soc. Amer.*, vol. 120, no. 5, pp. 2724–2736, Nov. 2006.

[10] P. Ioannides and C. A. Balanis, "Uniform circular and rectangular arrays for adaptive beamforming applications," *IEEE Antennas Wireless Propagat. Lett.*, vol. 4, pp. 351–354, 2005.

[11] Y. L. Ma, Y. Yang, Z. He, K. Yang, C. Sun, and Y. Wang, "Theoretical and practical solutions for high-order superdirectivity of circular sensor arrays," *IEEE Trans. Ind. Electron.*, vol. 60, pp. 203–209, 2013.

[12] H. H. Chen, S. C. Chan, and K. L. Ho, "Adaptive beamforming using frequency invariant uniform concentric circular arrays," *IEEE Trans.Circuits Syst. I, Reg. Papers*, vol. 54, no. 9, pp. 1938–1949, Sept. 2007.

[13] X. Zhang, W. Ser, Z. Zhang, and A. K. Krishna, "Selective frequency invariant uniform circular broadband beamformer," *EURASIP Journal on Advances in Signal Processing*, pp. 1–11, 2010.

[14] J. Benesty, J. Chen, and I. Cohen, *Design of Circular Differential Microphone Arrays*. Berlin, Germany: Springer-Verlag, 2015.

[15] Y. Buchris, I. Cohen, and J. Benesty, "Analysis and design of time-domain first-order circular differential microphone arrays," in *the 22nd International Congress on Acoustics (ICA)*, 2016.

[16] ——, "Frequency-domain design of asymmetric circular differential microphone arrays," *submitted to IEEE/ACM Trans. Audio, Speech, Language Process.*

[17] S. Doclo and M. Moonen, "Design of far-field and near-field broadband beamformers using eigenfilters," *Signal Process.*, vol. 83, pp. 2641–2673, Dec. 2003.

[18] L. Zhao, J. Benesty, and J. Chen, "Optimal design of directivity patterns for endfire linear microphone arrays," in *in Proc. IEEE Int. Conf. Acoust., Speech, Signal Process.*, 2015, pp. 295–299.

[19] J. Benesty, J. Chen, and C. Pan, *Fundamentals of Differential Beamforming*. Springer, 2016.